

Alloy Solutions to Metal Dusting Problems in the PetroChemical Industry

Brian A. Baker and Gaylord D. Smith, Special Metals Corporation, Huntington, WV, USA

Producing chemical derivatives of the refining process often involves the creation of a synthesized gas (syngas) stream consisting of a mixture of CO, H₂ and H₂O with lower levels of CO₂ and some CH₄. The synthesis and reducing gases derived by reforming processes are used as the basic feedstock in the production of plastics, synthetics, fertilizers, fibers and pharmaceuticals. When such gas mixtures are present in the process stream in the critical temperature range of about 400° to 800°C, the phenomenon labeled “metal dusting” can potentially be a severe corrosion problem. Past and present failures resulting from metal dusting have prompted end users and material producers alike to examine the causes of and potential solutions to this often-disastrous problem.

Metal dusting can be described as a catastrophic carburization phenomenon which occurs under conditions where the carbon activity of the gaseous atmosphere is greater than one. Metal dusting is manifested by the disintegration of the affected metal into a powdery mixture of graphite and metal particles. Oxides and carbides are also often present in the powdery mixture or 'dust'.

Special Metals corporation, which includes the business formerly known as Inco Alloys International, has been actively involved in characterizing and developing new materials to cope with the increasing demand on equipment in harsh metal dusting environments. Research has been conducted on a number of alloys, apart from the traditionally used primary and secondary reformer material INCOLOY® alloy 800H, to better understand the role of alloying in resisting attack. This article presents long term laboratory data and shows how the consideration of alloy content can be effective in resisting metal dusting attack.

Causes of Metal Dusting

The production of syngas from methane or natural gas via steam reforming is a common step to begin production of hydrogen, ammonia, methanol and liquid hydrocarbons (via Fischer Tropsch synthesis). The amount of steam used for the reforming process has been driven lower by the need for greater efficiency, resulting in lower steam-to-hydrogen ratios. Higher front-end pressures have also increased the CO content of the syngas. Lower H₂O/H₂ ratios in combination with higher CO/CO₂ ratios result in lower oxygen partial pressures and higher carbon activities, respectively, and serve to increase the severity of metal dusting attack. Metal dusting is often avoided in industry by designing around the critical metal dusting temperature range. Syngas is produced at temperatures above the critical range (>800°C) and transferred to a boiler via a short transfer line where it is rapidly quenched to temperatures below the critical metal dusting range (<400°C). Alloy ferrules that are used in the transfer line do often experience metal dusting and are periodically replaced. The need to maximize the efficiency of steam reforming technology has led to the development of equipment which must be capable of operating within the range of temperature and carbon activity which can promote metal dusting. This necessitates the use of materials which exhibit excellent resistance to metal dusting attack. Exploration of the range of conditions which produce metal dusting is being conducted intensively worldwide through consortia such as those coordinated by the Materials Technology Institute in the USA and the TNO Institute of Industrial Technology in Europe.¹

The mechanism of metal dusting for iron-base alloys begins with saturation of the alloy matrix with carbon/carbides, usually in a localized manner, and subsequent formation of metastable Fe₃C, or cementite. Decomposition of the cementite as the carbon activity approaches unity produces iron particles and powdery carbon. The metal particles then strongly catalyze further carbon deposition. A different mechanism is proposed for nickel-base alloys, which does not involve the formation of an intermediate metastable carbide. Such a mechanism begins in the same way as for iron-base alloys, with saturation of the alloy matrix with carbon/carbides. However, in the case of nickel-base alloys, the saturated matrix directly decomposes into metal particles and graphite.^{2,3} Figure 1 illustrates the equidistant diffusion (assuming a material which exhibits isotropic diffusion behavior) of carbon from a point defect in the protective oxide scale which results in saturation of a hemispherical region with carbon. Subsequent decomposition of this saturated area results in disintegration of the alloy matrix and not simply grain fallout, producing a pit having the same hemispherical shape as the carbon-saturated region.

Protection of an alloy against metal dusting attack requires the presence of an adherent, protective, healable oxide surface layer. While oxide formation may be stable, the oxide layer may still be susceptible to disruption. Higher levels of the scale forming element will then make the scale healing process more rapid and complete. Ultimate resistance to metal dusting may involve complex interactions of scale characteristics, diffusivity of scale-forming elements and carbon through the alloy matrix and carbon saturation limits.

Alloy Performance in Metal Dusting Environments

Changing processing conditions and the use of advanced catalysts have heightened the tendency of synthetic gas streams to promote metal dusting. Techniques such as injection of additional steam and sulfur-containing species into the gas stream, which are known to minimize the effects of metal dusting, are no longer viable in many processes due to the increased use of catalysts which are sensitive to sulfur content. Higher gas pressures and temperatures, in conjunction with lower H₂O/H₂ ratios and higher CO/CO₂ ratios are becoming the norm for modern reforming operations. This combination of conditions may necessitate the use of materials which offer resistance to metal dusting that is superior to that of previously commonly used alloys such as the Cr-Mo stainless steels and Fe-Ni-Cr alloys.

Two commonly used alloys that typically offer good overall corrosion resistance as well as high temperature strength under a wide range of conditions are INCONEL® alloy 600 and INCOLOY alloy 800H. Metal dusting failures of alloy 800 are well documented^{4,5} and problems with alloy 600 have been encountered as well. Figures 2 and 3 show metal dusting attack of both the alloy 600 piping and the alloy 800 connecting ring, respectively, from a reformer pigtail.⁶ The reformer had been in service for about 5 years. Harsher conditions have necessitated the use of alloys having high nickel contents in addition to higher levels of scale-forming elements, such as chromium. Alloy 601 has been used for waste heat boiler shells and tubing in ammonia plants as well as for reformer components and has resulted in greater production due to decreases in downtime and repair costs. For even greater protection against metal dusting under the harshest conditions, alloys such as INCOTHERM™ alloy TD, INCOLOY alloy MA956, INCOCLAD® 671/800HT and INCONEL alloy 617, INCONEL alloy 690, and INCONEL alloy 693, offer promising potential as an upgrade from the commonly used alloy 601.

Laboratory Testing

Table 1 shows the chemical composition for each alloy tested as well as for other alloys mentioned in this article. Test specimens were prepared from commercially available material; sample dimensions were approximately 2.5cm X 2.5cm X thickness. Samples were ground to a 120-grit finish for standardization purposes.

Exposures were performed at 621°C in an atmosphere generated from an inlet gas mixture of CO-20% H₂. Samples were cycled, lightly brushed and ultrasonically cleaned and mass change was measured at approximately two-week intervals. In addition to mass change, pitting depth was also determined for each sample using an optical microscope having a calibrated fine focus knob.

Figure 4 shows mass loss rates versus time for the alloys tested. The rate was calculated by dividing the mass change (only shown if negative) per unit area by the total test time. The maximum pit depth as a function of time is plotted in Figure 5. Figure 6 shows the result of multiple regression analysis of the log of the pit progression rate, calculated by averaging the pit depth over the total testing duration, versus the weight percentage of various alloying additions. Only the austenitic nickel-base alloys and Fe-Ni-Cr alloys were included in this calculation; the two ferritic alloys, MA956 and Fe-9Cr-1Mo, and also alloy 400 were excluded. The best fit was produced using the following summation:

$$\text{Log (Pit Progression Rate in } \mu\text{/h)} = (\% \text{Ni} + \% \text{Co}) + 5 * \% \text{Mo} + 20 * \% \text{Ti} + 33 * \% \text{Al} + 15 * \% \text{Si} + 2 * \% \text{Cr} - 2 * \% \text{Fe}.$$

This same regression technique was used to characterize the variation in mass loss rate with the percentage of certain alloying additions (Figure 7). Again, only the austenitic nickel-base and Fe-Ni-Cr alloys were included in the calculation. The best fit was obtained using the following summation:

$$\text{Log (Mass Loss Rate in mg/cm}^2\text{/h)} = 2 * (\% \text{Ni} + \% \text{Co}) + 6 * \% \text{Mo} + 31 * \% \text{Ti} + 34 * \% \text{Al} + 80 * \% \text{Si} + 9 * \% \text{Cr} - \% \text{Fe}.$$

As a general trend, nickel-base alloys exhibited lower mass loss rates and pitting progression rates than iron-base alloys. Exceptions include alloys 600 and MA754, which contain only 15% and 20% chromium and have no other significant additions of scale-forming or carbide-forming elements, and had a fairly high mass loss rate resulting from numerous, albeit fairly shallow, pits. Alloy 690 (Ni-29Cr-9Fe), commonly used as heat-exchanger tubing in the nuclear industry, exhibits much lower mass loss and pit progression rates than alloy 601 which is increasingly used as an upgrade from iron-base materials such as Cr-Mo steels, austenitic stainless steels and Fe-Ni-Cr heat-resistant alloys such as alloy 800. The mechanically alloyed corollary to alloy 690, alloy MA758, also exhibits good performance. Alloy MA956, a ferritic alumina former, also exhibited good performance. Alloy 263 performed well despite its modest chromium level of 20% and 39% iron content, and appears to possibly gain protection from its substantial titanium addition and possibly its molybdenum addition, which may promote early carbide formation and provide diffusional blocking of the carbon flux.⁷ Alloy 617, having 22% chromium and 1.2 aluminum, may also gain benefit from its molybdenum addition. Alloy 625 has performed reasonably well and contains 21.5% chromium, 9% molybdenum and 3.6% niobium. The new high silicon content of INCOTHERM alloy TD may have afforded some enhancement in performance, in addition to its 3% molybdenum content.

The INCONEL alloy 671 and alloy 693 show the highest performance in both resisting pitting attack and resisting mass loss, contain the highest combinations of nickel, chromium and aluminum. The protection of the material being enhanced by the very high level of scale-forming elements which form a dense, adherent and self healing protective oxide surface layer. Alloy 671, with its substantial chromium content, has performed well and could be utilized in the form of a bimetallic clad tube, being mechanically very poor as a monolithic material within the metal dusting temperature range. INCOCLAD tubes having an alloy 671 layer on the OD and alloy 800HT® at the ID have been successfully used in coal-fired boilers with service times exceeding 20 years. The best performer overall in the laboratory test was alloy 693, which possesses very high chromium and aluminum contents. In-situ field exposures in syngas environments have confirmed this alloy's superior performance.

Conclusion

Due to development of advanced catalysts and efforts to increase the efficiency of processes involving the production of syngas, metal dusting corrosion has become more prevalent. Failures of iron-base alloys as well as nickel-base alloys which contain insufficient scale-forming elements have prompted equipment designers to seek materials that are more resistant to metal dusting. Field and laboratory data confirm the desirability of addition of certain scale-forming and carbide-forming elements in conjunction with a nickel-base alloy matrix to limit pit progression rates.

Acknowledgements

The authors would like to thank Chad Clary for his assistance with laboratory testing and sample evaluation.

References:

- 1) R. T. Jones and K. L. Baumert, Paper No. 1372, CORROSION/2001, NACE International, 2001.
- 2) E. Pippel, J. Woltersdorf, R. Schneider, Materials and Corrosion, 49, 1998, pp 309-316.
- 3) H. J. Grabke, Materials and Corrosion, 49, 1998, pp 303-308.
- 4) Lai, G. Y., "High Temperature Corrosion of Engineering Alloys", ASM, 1990, pp 69-72.
- 5) "Handbook of Case Histories in Failure Analysis," Esaklul, K. A., ed., ASM, 1992, pp 351-353.
- 6) Private Communication, Special Metals, December, 1997.
- 7) S. Strauss and H. J. Grabke, Materials and Corrosion, 49, 1998, pp 321-327.

INCOCLAD®, INCONEL®, INCOLOY®, INCOTHERM™, MONEL®, NIMONIC® and 800HT® are trademarks of the Special Metals group of companies.

Alloy	Ni	Cr	Fe	Mn	Si	Al	Ti	C	Other
INCONEL® alloy MA754	78	20	-	-	-	0.3	0.5	0.05	0.5 Y ₂ O ₃
INCOTHERM™ alloy TD	73	22	-	-	1.4	-	-	0.01	3.0 Mo
INCONEL® alloy 600	72	15.5	8	0.3	0.3	0.3	0.3	0.08	-
INCONEL® alloy MA758	67	30	-	-	-	0.4	0.5	0.05	0.5 Y ₂ O ₃
MONEL® alloy 400	64	0.1	1.6	0.7	0.1	0.02	0.4	0.15	32.2 Cu
INCONEL® alloy 693	62	30	4	-	-	3	.3	-	-
INCONEL® alloy 625	61	21.5	2.5	-	0.1	0.2	0.2	0.02	9 Mo, 3.6 Nb
INCONEL® alloy 601	60.5	23	13	0.2	0.2	1.4	0.4	0.05	-
INCONEL® alloy 690	59	29	9	0.2	0.1	0.3	0.3	0.02	-
INCONEL® alloy 671	53	46	-	-	-	0.3	0.3	0.03	-
INCONEL® alloy 617	55	22	1	-	0.1	1.2	0.4	0.08	12.5 Co, 9 Mo
NIMONIC® alloy 263	51	20	39	0.3	0.1	0.5	2.2	0.06	20 Co, 5.9 Mo
INCOLOY® alloy 825	42	21.5	28	0.4	0.1	0.1	1	0.02	3 Mo, 2Cu
INCOLOY® alloy DS	37	16	41	1.0	2.3	-	-	0.08	-
INCOLOY® alloy 330	35	19	44	1.0	1.3	-	-	0.07	-
INCOLOY® alloy 803	34	27	36	1.0	0.8	0.4	0.4	0.08	-
INCOLOY® alloy 864	34	21	39	0.4	0.8	0.3	0.6	0.03	4.2 Mo
INCOLOY® alloy 800/800HT®	32	21	45	0.9	0.1	0.4	0.4	0.07	-
INCOLOY® alloy MA956	-	20	75	-	-	4.5	0.5	0.05	0.5 Y ₂ O ₃
9Cr-1Mo Steel	-	9	89	0.5	-	-	-	0.1	1 Mo

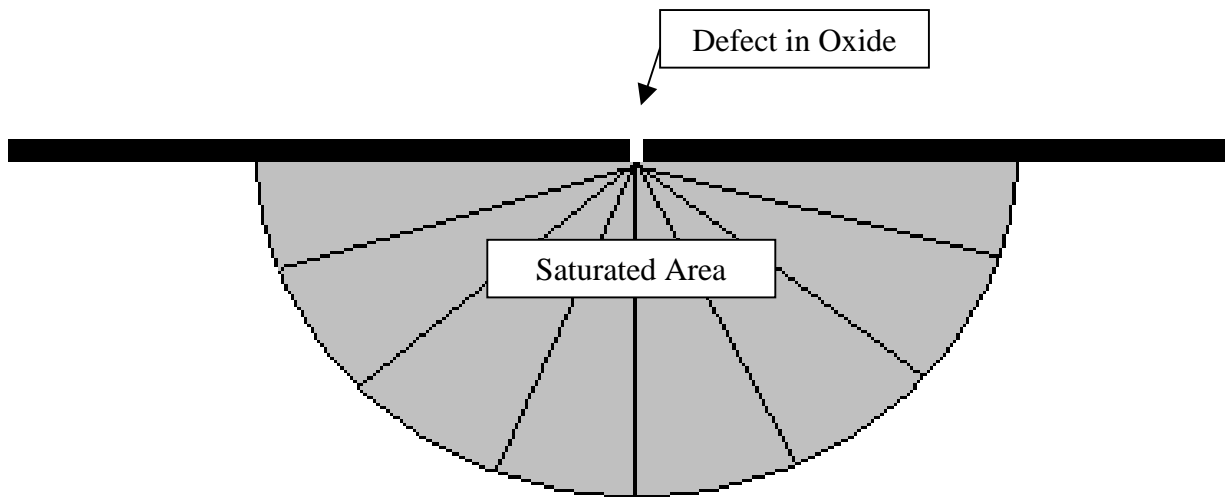


Figure 1. Illustration of the equidistant diffusion of carbon from a localized defect in the protective oxide scale that results in the saturation of a hemispherical region with carbon.

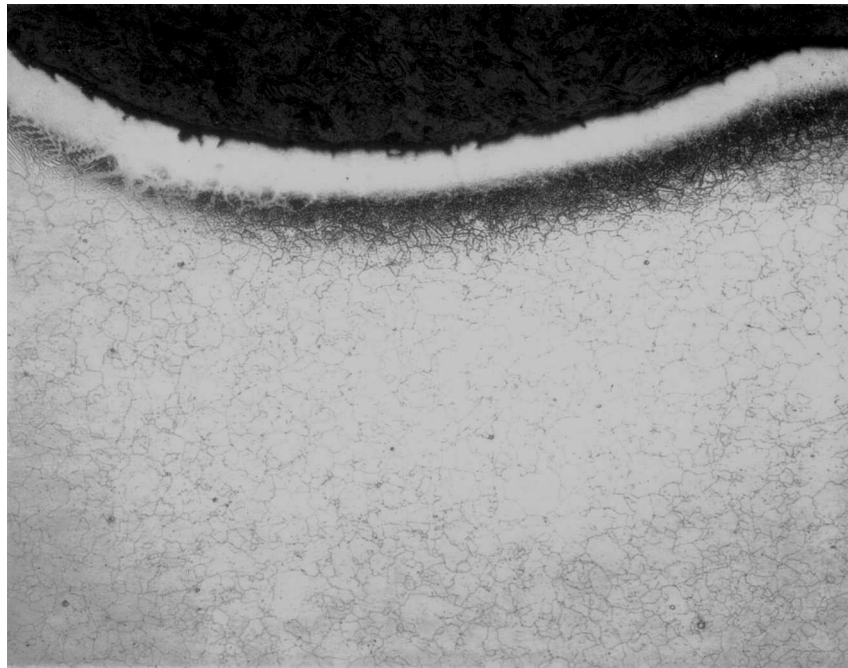


Figure 2. Photomicrograph showing cross section of metal dusting pit in alloy 600 reformer pigtail pipe which was in service for approximately 5 years. Etchant: 5% HNO_3 in methanol, electrolytic.

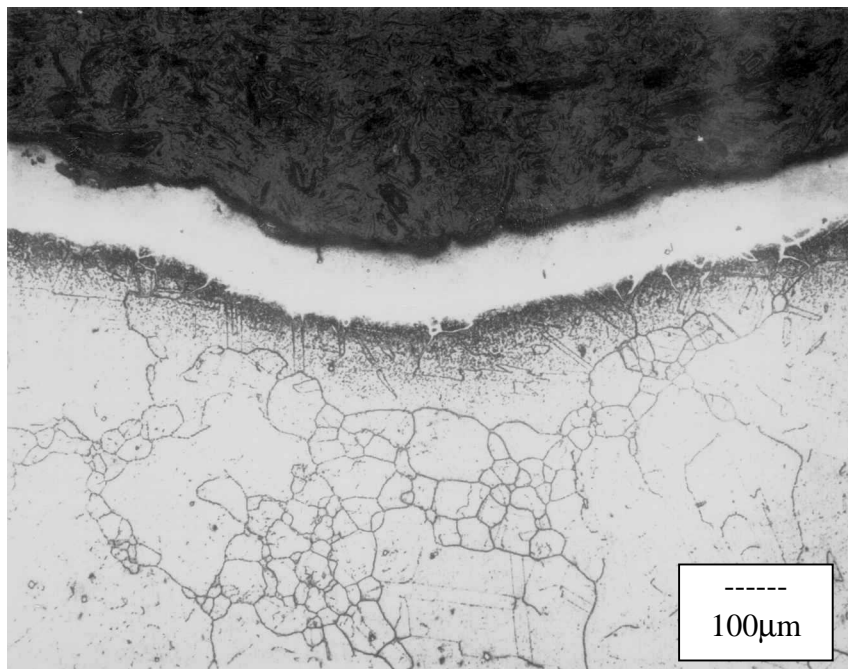


Figure 3. Photomicrograph showing cross section of metal dusting pit in alloy 800 reformer pigtail connecting ring which was in service for approximately 5 years. Etchant: 5% HNO_3 in methanol, electrolytic.

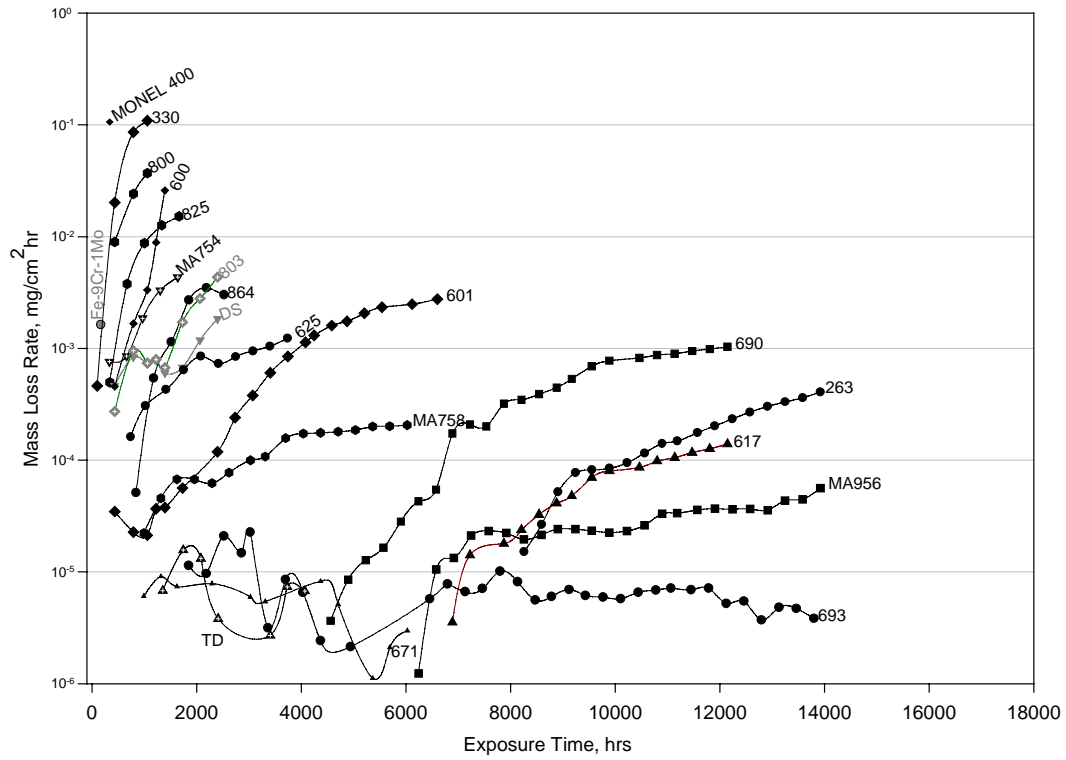


Figure 4. Mass loss rate versus exposure time for alloy samples exposed to CO-20% H₂ at 621°C.

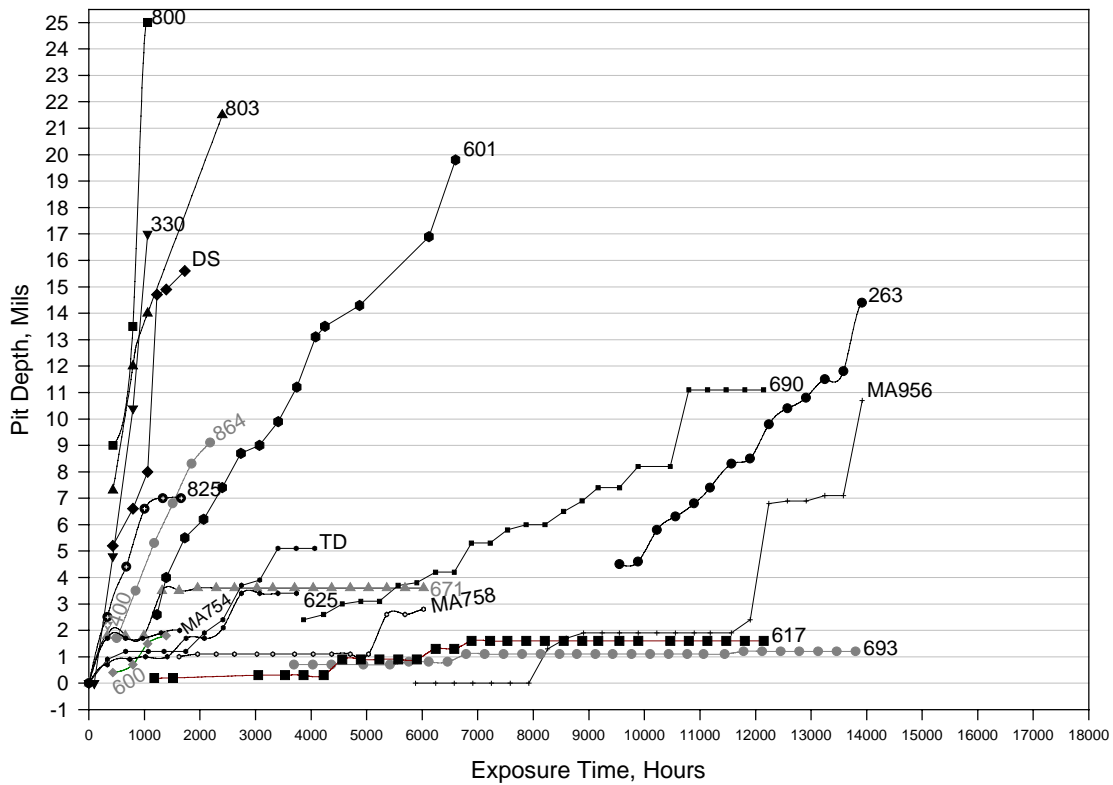


Figure 5. Maximum pit depth measurements for alloy samples exposed to CO-20% H₂ at 621°C.

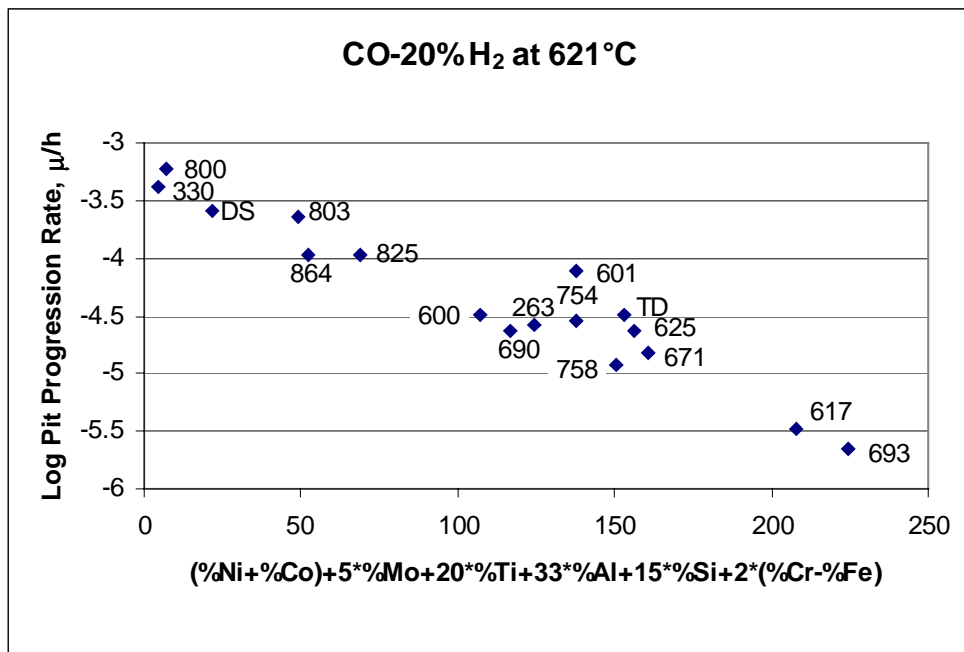


Figure 6. Results of multiple linear regression for pit progression rate.

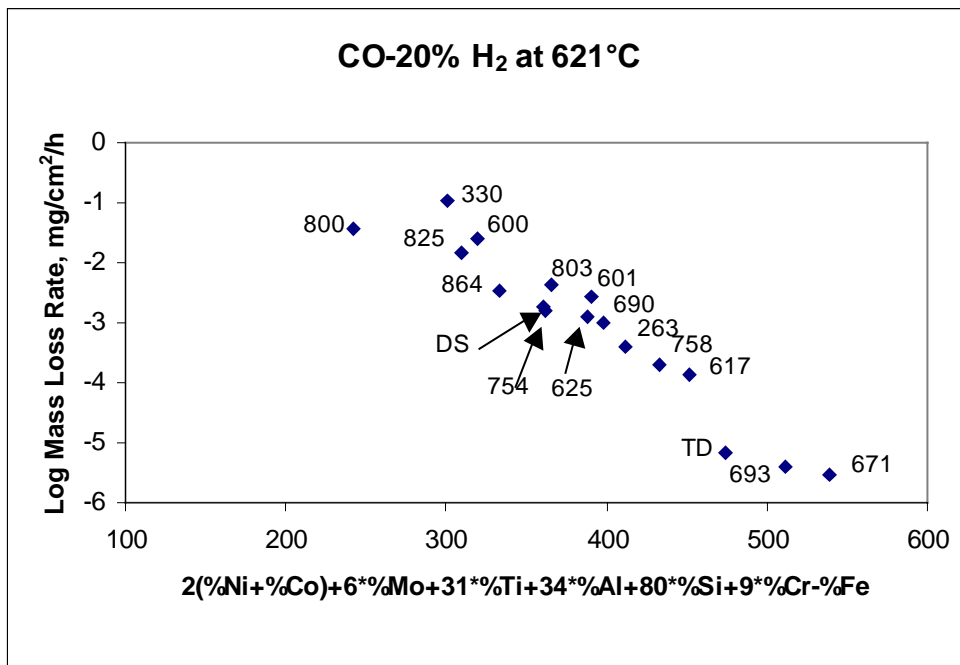


Figure 7. Results of multiple linear regression for mass loss rate.

